JOURNAL OF PHYSICAL ORGANIC CHEMISTRY
J. Phys. Org. Chem. 2001; **14:** 625–635
DOI:10.1002/poc.410

Deuterium conformational equilibrium isotope effects in 1,3,5-cycloheptatriene-7-*d*

Darón I. Freedberg,[1]* Max Kopelevich[2] and Frank A. L. Anet[2]

[1]Laboratory of Biophysics, CBER/FDA, 1401 Rockville Pike HFM-419, Rockville, MD 20852, USA
[2]Department of Chemistry and Biochemistry, University of California, Los Angeles, 405 Hilgard, Los Angeles, CA 90024, USA

Received 30 August 2000; revised 25 April 2001; accepted 1 May 2001

epoc ABSTRACT: We report a reinvestigation of the conformational equilibrium of 1,3,5-cycloheptatriene-7-*d* (CHT-7-*d*) by solution ^{1}H NMR at 500 MHz over a wide range of temperatures, and *ab initio* calculations up to the MP4 level. Lineshape analysis provided a barrier to ring inversion of approximately 6 kcal mol^{-1}. Equilibrium constants were measured in $CBrF_3$ and $CClF_2H$ by: integration when the ring-inversion rate is low; lineshape analysis when the ring-inversion rate is on the order of the chemical shift difference; and temperature-dependent chemical shift differences between CHT and CHT-7-*d* when the ring-inversion rate is fast. The three independent measurements confirm an equilibrium biased toward an equatorial deuterium, with $\Delta G^\circ = 52 \pm 8$ cal mol^{-1} (at $-173\,^\circ$C), $\Delta H^\circ = 55 \pm 8$ cal mol^{-1} and $\Delta S^\circ = 0.03 \pm 0.05$ cal mol^{-1} K^{-1} in $CBrF_3$. Supporting *ab initio* calculations yield: $\Delta H^\circ = 34$ cal mol^{-1}, $\Delta S^\circ = 0.014$ cal mol^{-1} K^{-1} (MP2/6-31G*); $\Delta H^\circ = 57$ cal mol^{-1} and $\Delta S^\circ = 0.03$ cal mol^{-1} K^{-1} (RHF/6-31G*); and a barrier to ring inversion in CHT of 4.26 kcal mol^{-1} (RHF/6-31G*), 9.76 kcal mol^{-1} (MP2/6-31G*), and 7.34 kcal mol^{-1} (MP4/6-31G* single point). The differences in calculated barrier heights due to exclusion or inclusion of Møller–Plesset energies indicate that the ground state is stabilized relative to the transition state at the MP2 and MP4 levels. This implies that homoconjugation is important in CHT, a neutral molecule. Our experimental values differ from those originally deduced by Jensen and Smith (*J. Am. Chem. Soc*. 1964; **86**: 956): $\Delta G^\circ = 72$ cal mol^{-1}, $\Delta H^\circ = 142 \pm 30$ cal mol^{-1} and $\Delta S^\circ = 0.7 \pm 0.3$ cal mol^{-1} K^{-1}.
Additional material for this paper is available from the epoc website at http://www.wiley.com/epoc

KEYWORDS: deuterium; conformational isotope effect; cycloheptatriene; homoaromaticity; *ab initio*; NMR

INTRODUCTION

'Tropilidene' or 1,3,5-cycloheptatriene (CHT) was first isolated by Ladenburg in 1883,[1] and has challenged organic chemists since. One important feature of CHT is that it is fluxional, i.e. it is in rapid equilibrium, even well below room temperature, with its bicyclic isomer, bicyclo[4.1.0]hepta-2,4-diene, or norcaradiene (NCD). This fluxionality was not recognized in early work, and has direct relevance to the present study of CHT ring inversion because the amount of NCD present affects the interpretation of results obtained for CHT. The studies by Rubin[2] and Miura[3] imply that NCD is less stable than CHT by about 4 to 6.5 kcal mol^{-1}, though a recent report suggests that a solution of CHT may contain as much as 2% NCD at room temperature.[4] Many of the simple derivatives of CHT and NCD exist with the equilibrium biased toward the CHT form.[3] Yet, in some reactions with dienophiles, all the products obtained are due to the tiny equilibrium amount of NCD.[5]

NCD and CHT are related because they are homoaromatic[6] with respect to benzene. As Winstein proposed (Fig. 1),[6] the replacement of a carbon–carbon single bond (as opposed to a double bond) in benzene by a CH_2 group gives rise to CHT, a σ homoaromatic analog of benzene; the replacement of a π-bond in benzene by a CH_2 group produces NCD, a π homoaromatic analog of benzene. For homoaromaticity to be effective, CHT should be boat shaped so that the p orbitals on C-1 and C-6 can overlap to form a six-electron pseudo-cyclic system. This overlap decreases the C1—C6 distance, hence homoaromaticity can distort the CHT structure towards the NCD structure. It is not unreasonable to suggest that the overlap could also stabilize the ground state, and thus may increase the ring-inversion barrier in CHT. We have obtained evidence of p-orbital overlap between C1 and C6 from *ab initio* calculations, and explore its structural consequences by examining the ring-inversion equilibrium in CHT.

Before describing the motivation behind the ring inversion investigation, we briefly outline the relevant

**Correspondence to:* D. I. Freedberg, Laboratory of Biophysics, CBER/FDA, 1401 Rockville Pike HFM-419, Rockville, MD 20852, USA.
E-mail: freedberg@cber.fda.gov

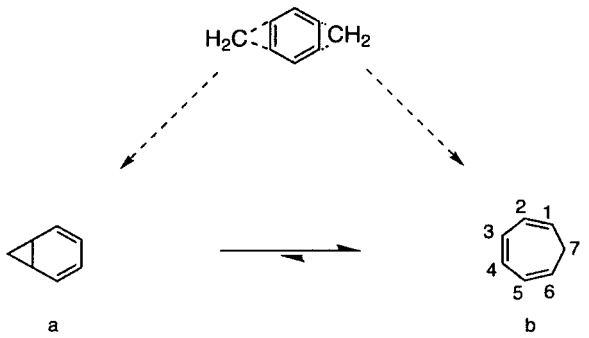

Figure 1. The relationship between NCD (a) and CHT (b). Addition of a CH_2 group in across a π bond in benzene produces NCD, whereas addition of CH_2 group across a σ bond in benzene produces CHT

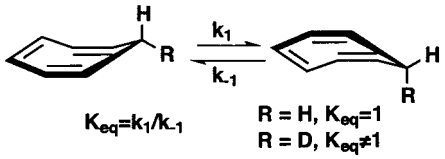

Figure 2. Figure depicting the equilibrium in CHT. Note that the equilibrium is degenerate when R=H; however, when R=D the equilibrium is biased[12] toward the conformer with an equatorial deuterium

history of CHT structural studies. Corey et al.[7] used ^{1}H NMR to distinguish NCD from CHT in 'troplidene'. They concluded that the equilibrium, in what was then called 'tropilidene', is heavily skewed toward CHT. Interestingly, their data are consistent with up to 10% NCD present in solution. This NMR study did not address the planarity or non-planarity of CHT, and direct structure determination is difficult because CHT is a liquid. Consequently, subsequent structural work relied on indirect evidence to determine whether CHT is planar or boat shaped. Electron diffraction[8] and microwave studies[9] of CHT, as well as X-ray studies of thujic acid,[10] a derivative of CHT, implied that CHT is non-planar. In 1963 la Lau and de Ruyter[11] reported that the IR spectrum of 1,3,5-cycloheptatriene-7-*d* (CHT-7-*d*) showed two stretching bands, which strongly suggests that there are two types of bond at the methylene position in CHT-7-*d*, and that the carbon skeleton of CHT is boat shaped. Short of an X-ray study on CHT at very low temperatures, the best method to establish the three-dimensional structure of CHT is *ab initio* calculations.

In 1964 Jensen and Smith[12] and Anet[13] demonstrated that CHT is boat shaped and is associated with a degenerate ring-inversion equilibrium (see Fig. 2). The free energy barrier to ring inversion in CHT of 5.7 kcal mol^{-1} (in $CBrF_3$),[12] and 6.3 kcal mol^{-1} (in CF_2Cl_2)[13] was measured by low-temperature ^{1}H NMR. Under conditions of slow ring-inversion, the aliphatic region of the spectrum showed two peaks, one for the axial and one for the equatorial proton of CHT. Jensen and Smith[12] assigned these peaks in the slow exchange using CHT-7-*d*, and reported that CHT-7-*d* showed an equatorial preference for deuterium from direct integration of the axial and equatorial peaks. The relative areas under the axial and equatorial peaks of the CHD group in CHT varied with temperature, and thus were used to measure the temperature dependence of $\Delta G°$ between -168 and -158 °C. Above the coalescence temperature, the CHD group shows a single broad peak, whose chemical shift is the population weighted average of the shifts of the axial and equatorial protons. Thus, K_{eq} (and $\Delta G°$) can be calculated above the coalescence temperatures. Jensen and Smith's measurements were the first observation of an equilibrium chemical shift isotope effect.[14] In this case the deuterium also has an intrinsic isotope effect on the proton chemical shift in the CHD group.[14–16] But the more interesting equilibrium isotope effect perturbs the chemical shift indirectly by biasing an equilibrium that, in the absence of deuterium (as in CHT itself), is degenerate. Later, Saunders and, subsequently, others showed that equilibrium isotope effects are delicate tools with wide applicability in the study of rapidly equilibrating carbocations and the conformations of both cyclic and acyclic molecules.[17–27] Jensen and Smith[12] also reported that $\Delta H° = 134 \pm 30$ cal mol^{-1}, and $\Delta S° = 0.7 \pm 0.3$ cal mol^{-1} K^{-1} for the ring-inversion equilibrium in CHT-7-*d*. This unexpectedly large $\Delta S°$ predicts that, although the equilibrium in CHT-7-*d* is biased toward an equatorial deuterium at low temperatures, the conformational preference switches to an axial deuterium above 191 K.[28,29] The reported $\Delta G°$ values are reliable, but they contain systematic errors that lead to large correlated errors when used to extract $\Delta H°$ and $\Delta S°$. In this paper we report a reinvestigation of the isotope effect in, and structure of, CHT using modern NMR instrumentation and *ab initio* calculations. We also consider the implications of homoaromaticity in CHT on the ring-inversion equilibrium and the CHT–NCD equilibrium.

EXPERIMENTAL METHODS

Synthesis

CHT-7-*d* was prepared in a manner similar to Conrow's method.[30] 10 ml each of pentane and D_2O (99% Cambridge Isotope Laboratory) were combined in a 25 ml round-bottom flask equipped with a stirbar and cooled to 0 °C. To this stirred, biphasic solution were added 0.497 g (11.88 mmol) $NaBD_4$ (99.95% isotopic purity, Cambridge Isotope Laboratory), followed by slow addition of 1.106 g (6.22 mmol) tropylium fluoroborate, $C_7H_7BF_4$ (Aldrich), using a porcelain spatula. The mixture was allowed to stir overnight. Excess $NaBD_4$ was quenched with a 37% aqueous formaldehyde solution. The aqueous

layer was extracted with pentane, and the combined organic layers were dried ($MgSO_4$) and filtered. The CHT-7-*d* solution in pentane was concentrated on a rotary evaporator and the remaining CHT was purified by preparative gas chromatography on a silicon (SE-30) column at 80 °C.

NMR sample preparation

The thin end of a Pasteur pipet, containing a small amount of the sample, was placed in an NMR tube immersed in a dry-ice/dichloromethane bath (−78 °C). Because a pressure regulator was not available, Freon solvent ($CBrF_3$ or $CClF_2H$) was removed from a liquefied gas-cylinder into a balloon through a piece of Tygon tubing. The Tygon tubing (connected to the balloon) was attached to the pipet and the gas slowly condensed into the NMR tube, dissolving the compound present at the bottom of the pipet. The tube was capped and kept in a dry-ice/dichloromethane bath until inserted into a pre-cooled NMR probe.

NMR studies

^{1}H NMR studies of CHT and CHT-7-*d* were carried out in two different solvents, $CBrF_3$ (Matheson) and $CClF_2H$ (Du-Pont). ^{1}H NMR measurements were recorded on a Bruker AM500 spectrometer operating at 500.135 MHz using a probe equipped with orthogonal ^{1}H–^{19}F coils. A fluorine frequency was used to lock on the Freon solvent signal. The sample tube was inserted into the probe only after the probe had been pre-cooled to −62 °C for samples dissolved in $CBrF_3$, or −51 °C for samples dissolved in $CClF_2H$.

Variable-temperature measurements were performed using a Bruker BVT-1000 temperature controller and a home-built copper heat-exchange coil immersed in liquid nitrogen (contained in a 25 l Dewar vessel) through which nitrogen gas flowed to cool the probe. Cold nitrogen gas from the coil flowed to the probe *via* Tygon tubing insulated with cotton wool and foam-rubber. The probe thermocouple was calibrated by plotting temperature readings, from the BVT-1000 unit, against sample temperatures measured from methyl–OH chemical shift differences.[31] These points were fitted to a line and the correction to the thermometer readings was extrapolated to low temperatures.

The Freon ^{1}H signal in $CClF_2H$ was suppressed using presaturation. Slow-exchange NMR spectra were acquired with a pulse program; this generated two spectra, 90° out of phase with respect to one another. The two spectra were processed with a Lorentz-to-Gauss transformation and a matched filter, phased, and then added together to eliminate the dispersive tails that occur in real-Fourier-transform spectra.[32] Zero-order (vertical offset) and first-order (linear) baseline corrections were applied in order to avoid baseline slope, which would cause errors in the integration data measured at low temperatures. Higher-order baseline corrections were deliberately not applied.

In low-temperature integration measurements employing $CBrF_3$, homonuclear gated decoupling of the α vinylic protons in CHT-7-*d* was used in order to obtain the sharpest possible lines for the axial and equatorial protons. The decoupler was gated off during the relaxation delay prior to the transmitter pulse to avoid any perturbation of the peak areas by unwanted nuclear Overhauser effects.[33]

Extraction of thermodynamic parameters

Thermodynamic parameters for CHT-7-*d* were measured between −175 and −65 °C in $CBrF_3$ and between −110 and −51 °C in $CClF_2H$. Thermodynamic data from the NMR spectra can be obtained in the slow-, intermediate- and fast-exchange regions.

Slow-exchange region (below −145 °C). Equilibrium constants were measured directly in the slow-exchange region in a sample containing only pure CHT-7-*d* by integrating the area under the separate axial and equatorial proton signals in the ^{1}H NMR spectrum. Integration yielded equilibrium constants that were then converted to free-energy differences.

Intermediate-exchange region (−145 to −110 °C). The sample used to measure these spectra contained pure CHT-7-*d*. Experimental spectra were measured at −140 °C, and worked up using an exponential multiplier with 20 Hz line broadening, to increase the signal-to-noise ratio. They were analyzed using a program that simulates the two-site exchange in CHT-7-*d* as the sum of three, two-site dynamic NMR exchange spectra, which correspond to a two-site exchange for two triplets. The total line shape depends on the axial–equatorial chemical shift difference, the equilibrium constant, and the rate constant for ring inversion in either direction.[34] The total line shape was simulated to give line widths and peak areas, which were converted into equilibrium constants.

Fast-exchange region (above −110 °C). A sample with a 5:1 ratio of CHT-7-*d*:CHT was used to extract equilibrium constants in fast exchange. This was accomplished by measuring the difference in the averaged chemical shift between the ^{1}H resonance of the CH_2 group in CHT and the ^{1}H resonance of the CHD group in CHT-7-*d* in the fast-exchange region.

The averaged chemical shift for CHT in fast-exchange

can be written as:

$$\delta_H = \frac{1}{2}(\delta_a + \delta_e) \quad (1)$$

where δ_a and δ_e are the ^{1}H NMR chemical shifts for the axial and equatorial hydrogen atoms respectively in the absence of exchange.

In general, there will be a two-bond intrinsic isotope effect (IIE) on the ^{1}H chemical shift in substituting a CHD for a CH_2 group; δ_a' and δ_e' include the intrinsic isotope effect of the deuterium atom on the proton's chemical shift using the following equations:

$$\delta_a' = \delta_a + {}^2\Delta_a$$
$$\delta_e' = \delta_e + {}^2\Delta_e \quad (2)$$

where $^2\Delta_a$ and $^2\Delta_e$ are the two-bond IIE's on the axial and equatorial protons, respectively.

Equation (3) describes the averaged chemical shift, δ_D, of the ^{1}H resonance of the CHD group in CHT-7-*d* in terms of the axial and equatorial fractional populations, p_a and p_e, respectively.

$$\delta_D = p_e\delta_a' + p_a\delta_e' \quad (3)$$

The equilibrium constant K_{eq} for this exchange in CHT-7-*d* can be written as

$$K_{eq} = p_a/p_e \quad (4)$$

If CHT is the only species present, p_a and p_e are fractional populations, their sum must by definition be equal to one. Using the relation $p_a + p_e = 1$ and Eqn. (4), we can write two new expressions, which separately relate the axial and equatorial populations to the equilibrium constant.

$$p_e = 1/(1 + K_{eq}) \quad \text{and} \quad p_a = K_{eq}/(1 + K_{eq}) \quad (5)$$

Using Eqns ((1)–(3)) and (5), the difference $\Delta\delta$ between the averaged proton chemical shifts of the CHT and CHT-7-*d* methylene group is given by:

$$\begin{aligned}\Delta\delta &= \delta_D - \delta_H \\ &= 1/2(K_{eq} - 1/K_{eq} + 1)(\delta_e - \delta_a) \\ &\quad + [1/(K_{eq} + 1)](K_{eq}{}^2\Delta_a + {}^2\Delta_e)\end{aligned} \quad (6)$$

Equation (6) can be rearranged to give:

$$\begin{aligned}K_{eq} &= [1 - 2(\Delta\delta - {}^2\Delta_e)]/[(\delta_e - \delta_a)] \\ &\quad /[1 + 2(\Delta\delta - {}^2\Delta_a)/(\delta_e - \delta_a)]\end{aligned} \quad (7)$$

The difference between the averaged CHT and CHT-7-*d* methylene ^{1}H chemical shifts, $\Delta\delta$, is expected to be approximately 30 Hz at 500 MHz (60 ppb); $^2\Delta_a$ and $^2\Delta_e$ are expected to be 9 Hz at 500 MHz (18 ppb). The values of $\Delta\delta$, $^2\Delta_a$ and $^2\Delta_e$ are small compared with $\delta_e - \delta_a$, which is approximately 700 Hz (1400 ppb), thus the terms $(\Delta\delta - {}^2\Delta_e)/(\delta_e - \delta_a)$ and $(\Delta\delta - {}^2\Delta_a)/(\delta_e - \delta_a) \ll 1$. The binomial theorem can then be used to expand the denominator in Eqn. (7). Keeping only the lowest term gives:

$$\begin{aligned}K_{eq} &= 1 - 4[\Delta\delta/(\delta_e - \delta_a)] \\ &\quad - 2[({}^2\Delta_a + {}^2\Delta_e)/(\delta_e - \delta_a)]\end{aligned} \quad (8)$$

Since the overall intrinsic isotope effect in the fast-exchange region is the average of $^2\Delta_e$ and $^2\Delta_a$ we may substitute $^2\Delta_{int} = 1/2\ (^2\Delta_e + {}^2\Delta_a)$ into Eqn. (8) to yield:

$$K_{eq} = 1 - 4[(\Delta\delta - {}^2\Delta_{int})/(\delta_e - \delta_a)] \quad (9)$$

Equation (9) relates the equilibrium constant in the fast-exchange region to the difference between the observed CHT and CHT-7-*d* methylene proton chemical shifts, $\Delta\delta$, and to the axial-H equatorial-H chemical shift difference, $\delta_e - \delta_a$, in the absence of exchange at the same temperature. The $\delta_e - \delta_a$ term cannot, in practice, be measured directly in the fast-exchange region, but it can be extrapolated from the chemical-shift difference measured in the slow-exchange region.

Before purifying CHT-7-*d* by gas chromatography, a test of CHT was run. Consequently, the sample of CHT-7-*d* in $CBrF_3$ used in the low-temperature integration study contained a small amount of CHT contamination, which was easily visible in the fast-exchange region. At −70 °C, the lines of the two isotopomers are sharp and well separated because of both an intrinsic isotope effect and an isotope effect on the averaged chemical shift. The fraction *f* of CHT to CHT-7-*d* was found to be 1/9 by integration of the two signals. At temperatures between −148 and −175 °C, where integrals were measured, the methylene ^{1}H resonances for the two isotopomers overlap, but the integrals can be corrected for the (non-deuterated) CHT present. The measured peak area ratio *R* is an apparent equilibrium constant that is related to the true equilibrium constant K_{eq} as shown in Eqn. (10):

$$K_{eq} = \left[R\left(1 + \frac{f}{2}\right) - \frac{f}{2}\right] \Big/ \left[1 + \frac{f}{2}(1 - R)\right] \quad (10)$$

Computational methodology

To complement experimental NMR measurements the geometry of CHT was optimized and vibrational frequencies were calculated with *ab initio* quantum mechanical calculations. The geometry of CHT was optimized at the RHF/3-21G, RHF/6-31G*, RHF/6-311G* and MP2/6-31G* with Gaussian 92.[35] For each level of theory employed, vibrational frequencies were

Table 1. Thermodynamic parameters and chemical shits of CHT-7-*d* measured at low temperatures by NMR

Temperature (°C)	$\delta_e - \delta_a$ (Hz)	Observed ratio[a]	Corrected ratio	K_{eq}	$\Delta G°$ (cal mol^{-1})
−155.3[c]	712.0[c]	0.833 ± 0.018	0.809 ± 0.018	0.81 ± 0.02	51.5 ± 6
−165.0[c]	724.6[c]	0.826 ± 0.018	0.801 ± 0.018	0.80 ± 0.02	49.6 ± 6
−170.7[c]	732.6[c]	0.750 ± 0.045	0.779 ± 0.045	0.78 ± 0.05	51.3 ± 13
−173.5[c]	736.1[c]	0.769 ± 0.055	0.737 ± 0.055	0.74 ± 0.06	60.2 ± 16
−140.2[b]	765.0[b]	nd	nd	nd	nd
−149.2[b]	771.3[b]	nd	nd	nd	nd
−157.3[b]	778.4[b]	nd	nd	nd	nd
−168.8[b]	786.8[b]	nd	nd	nd	nd
−175.4[b]	791.2[b]	nd	nd	nd	nd

nd = no data.
[a] Equatorial H: axial H.
[b] Measured in $CClF_2H$.
[c] Measured in $CBrF_3$.

calculated after the complete geometry was optimized. Subsequent to the frequency calculations for the undeuterated molecule, the conformational isotope effects in the two C_s forms of CHT-7-*d* were calculated with the *readiso* function, which uses the mass-weighted, diagonalized, second derivative (Hessian) matrix to calculate vibrational frequencies in isotopically substituted molecules. Equations governing extraction of thermodynamic parameters can be derived from the Bigeleisen formalism;[29,36] however, excitation of the modes is probably a minor factor. As a result, $H°$ was extracted from calculated values of E and ZPE as follows: $H° = E° - \text{ZPE}$ ($\Delta H° = H°_{eq} - H°_{ax}$), and $\Delta S°$ was calculated from $S°$, which is directly available in the output of Gaussian. All calculations were performed at the UCLA Office of Academic Computing (OAC) on an IBM ES/9000 model 900 computer.

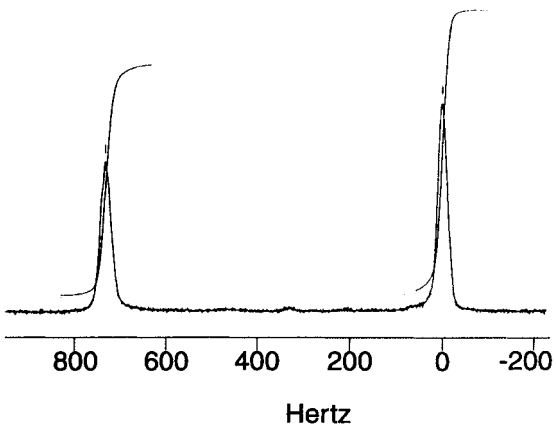

Figure 3. A typical ^{1}H NMR spectrum of CHT-7-*d* at −173.5 °C. The spectrum shows two separate peaks one (upfield) for the axial, and one (downfield) for the equatorial hydrogen atom in CHT-7-*d*, and a flat baseline. Integration of these two peaks yields a larger area for the axial proton and implies that the equilibrium in CHT-7-*d* is biased towards an equatorial deuterium

RESULTS AND DISCUSSION

Figure 3 shows a typical spectrum of CHT-7-*d* in $CBrF_3$ at −173.5 °C. For temperatures between −174 and −151 °C, the peaks arising from the axial and equatorial hydrogens are separated by at least 712 Hz, and the area under each peak can be integrated. Data obtained in the slow-exchange region by integration of the (more shielded) and axial (less shielded) equatorial C—H resonances in CHT-7-*d* in $CBrF_3$ are shown in Table 1. Each of these data points is the average of 16 individual measurements, and errors are reported to 95% confidence limits.[37] The integrals, and hence the values of K_{eq} measured at −155.3, −165.0, and −170.7 °C in $CBrF_3$ do not show significant temperature dependence. Standard deviations in the integration data at higher temperatures are 2% (−155.3, −165.0 °C), and increase to 6% for lower temperatures (−170.7 and −173.5 °C), slightly higher than the fractional errors reported by Jensen and Smith. The present measurements indicate that the values obtained by Jensen and Smith[12] are reproducible, and support the conclusion that in CHT-7-*d* the equilibrium is biased toward an equatorial deuterium. Although the integrated ratio at −173.5 °C deviates somewhat from the ratios measured at higher temperatures in slow exchange, the large uncertainty in the measurement of this data point puts it within experimental error of the other values measured in the slow exchange. The larger errors indicate that, at extremely low temperatures, accurately measuring integrals is challenging, even in the presence of flat spectral baselines. The equilibrium constants yield $\Delta G°$, which is relatively constant from −173.5 to −155.3 °C (Table 1). It is noteworthy that obtaining $\Delta H°$ and $\Delta S°$ from these measurements alone may result in large systematic errors, because the data were measured using only integration over a small temperature range. To avoid this complication, $\Delta H°$ and $\Delta S°$ were extracted using two independent techniques over 110 °C. Together, low-temperature integration and Saunders' isotopic perturbation method minimize systematic errors.

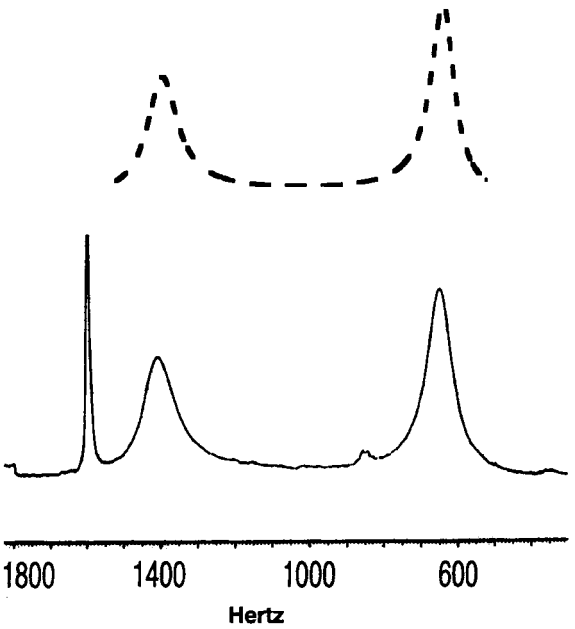

Figure 4. Total lineshape simulation (upper trace) of CHT-7-*d* at −140 °C in a mixture of $CClF_2H$ and $CDFCl_2$ in the intermediate exchange region, and experimental spectrum (lower trace). The sharp peak, whose linewidth remained constant at all temperatures, is attributed to EDTA present in trace amounts in the double-ended needle used for solvent-transfer. Fitting the experimental spectrum yields $\delta_e - \delta_a$ difference of 765 Hz, and forward and backward rate constants of $k_1 = 189\ s^{-1}$ and $k_{-1} = 246\ s^{-1}$ respectively, and $K_{eq} = 0.77$

Figure 4 shows the measured and calculated NMR spectra at −140 °C in $CClF_2H$. The signals are too broad to integrate accurately as there is a small, but significant overlap of the axial and equatorial ^1H resonances due to exchange. The experimental spectra were fit by varying the adjustable parameters in the total line-shape program. Fitting of the intermediate-exchange ^1H NMR spectrum obtained at −140 °C gave a chemical shift difference, $\delta_e - \delta_a$, of 765 Hz, and forward and backward rate constants of $k_1 = 189\ s^{-1}$ and $k_{-1} = 246\ s^{-1}$ respectively (for the equilibrium written as in Fig. 2). The corresponding free energies of activation, $\Delta G_1^{\ddagger}$ and $\Delta G_{-1}^{\ddagger}$, are 6.2 kcal mol^{-1} and 6.1 kcal mol^{-1} respectively. The equilibrium constant K_{eq} is 0.77, with the equilibrium biased towards an equatorial deuterium. This corresponds to a free energy difference of 69 cal mol^{-1} at −140 °C. The $\Delta G°$ value obtained from this spectrum has a large error because the equilibrium constant obtained in fitting this spectrum depends on the spectral baseline being flat under broad, overlapped peaks. An error in baseline calculation could yield inaccurate peak intensities, and thus introduce errors in values of $\Delta G°$. Such an analysis is prone to error whose magnitude is difficult to calculate. By comparison with integration and high-temperature data in Tables 1 and 2, the errors in $\Delta G°$ must be large (approximately ±15–20 cal mol). However, the rate constant k is used to calculate $\Delta G^{\ddagger}$, *via* ln(k), and even substantial errors in k are immaterial.

Table 2. Equilibrium constants in the fast-exchange limit as measured by NMR

Temperature (°C)	$\Delta\delta$ (Hz)	$\delta_e - \delta_a$ (Hz)[a]	K_{eq}
−51.2[b]	30.59[b]	716.2 ± 30[b]	0.89 ± 0.07[b]
−71.2[b]	33.69[b]	725.6 ± 26[b]	0.88 ± 0.07[b]
−90.7[b]	37.57[b]	735.3 ± 18[b]	0.86 ± 0.06[b]
−100.7[b]	38.34[b]	740.7 ± 15[b]	0.86 ± 0.06[b]
−65.2[c]	28.47[c]	609.28 ± 13[c]	0.887 ± 0.07[c]
−77.9[c]	30.18[c]	622.33 ± 12[c]	0.880 ± 0.06[c]
−87.7[c]	31.82[c]	632.71 ± 9[c]	0.873 ± 0.06[c]
−97.2[c]	33.57[c]	640.16 ± 8[c]	0.866 ± 0.06[c]
−107.2[c]	35.32[c]	653.30 ± 7[c]	0.860 ± 0.05[c]

[a] Extrapolated using Eqn. (11).
[b] Measured in $CClF_2H$.
[c] Measured in $CBrF_3$.

Figure 5 shows a typical ^1H NMR spectrum of a mixture of CHT and CHT-7-*d* in $CBrF_3$ at −87.7 °C. In the fast-exchange region two signals are observed: an upfield resonance for the CHD (axial and equatorial) protons, and a downfield resonance for the CH_2 protons. There is a measurable, temperature-dependent chemical shift difference between these two signals, and this difference provides the means to calculate an equilibrium constant at each temperature where fast-exchange spectra are measured (Table 2). Equation (9) requires the axial–equatorial chemical shift difference, which is not directly measurable in the fast-exchange region.

Axial–equatorial chemical shift differences in fast-exchange (Table 2) can be obtained through extrapolation of the temperature dependence of the chemical shift

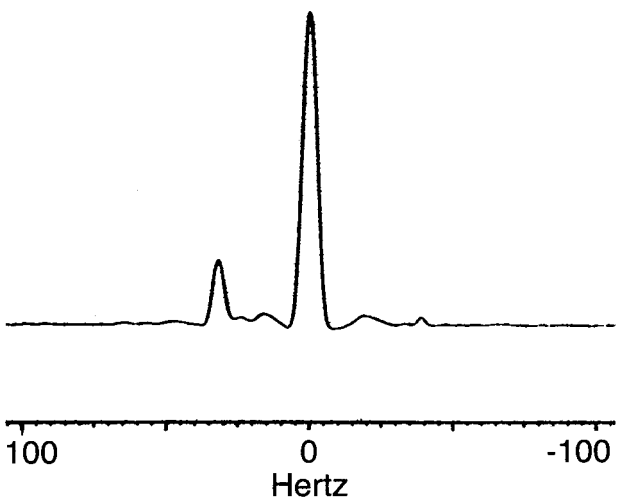

Figure 5. Fast-exchange ^1H NMR spectrum of a mixture of CHT and CHT-7-*d* in $CBrF_3$, at −87.7 °C. The difference in chemical shifts arises because the equilibrium of CHT-7-*d* is biased, whereas in CHT it is degenerate

difference measured in the slow exchange. At this point, a model that properly reproduced the observed temperature dependence of the CHD ^{1}H chemical shifts was needed. This task was complicated by the fact that in CHT-7-*d* the chemical shift differences in the slow-exchange region show a significant temperature dependence, and, therefore, any small errors will be amplified through extrapolation. In fitting the chemical shifts to temperature, all available information about this dependence was considered. A function that models the temperature dependence of the chemical shifts should have no discontinuities or unexpected features, and should have similar values in nearby temperature intervals. Clearly, it is best to model the temperature dependence of these chemical shifts with the simplest possible expression. The simplest would be a fit to a straight line, where the shifts diverge at infinite temperature. The fit can also be done with respect to inverse temperature; the results then diverge at 0 K.

A more complex model, which exhibits better limiting values of the chemical shifts than the ones discussed above, was also investigated. The temperature dependence of the chemical shifts was modeled by allowing $\delta_e - \delta_a$ to approach limiting values at both low and high temperatures. The function

$$\delta_e - \delta_a = a - \left[\frac{bT}{(1 + T/c)}\right] \qquad (11)$$

where a and b are in hertz, and c is a parameter in kelvin that influences the curvature of the line, models the behavior described above (note that when c is very large, a straight line is obtained). When the temperature T is small, $\delta_e - \delta_a$ approaches a, which is a constant for a given value of c. At high temperatures, $\delta_e - \delta_a$ approaches $a - b$. In carrying out the fits, c was entered manually, whereas the values for a and b were optimized in Igor[38] to fit the data points. We found that the data in $CBrF_3$ fit equally well when $c = 250$ K ($\chi^2 = 1.41$) or 500 K ($\chi^2 = 1.86$), and when $c = 500$ K ($\chi^2 = 1.92$) in $CClF_2H$.

Equation (11) provides reasonable fits to the axial equatorial chemical shift difference in CHT-7-*d* (supplementary figure S1). In order to estimate the error in fitting these points to Eqn. (11), curves fit to the data with $c = 100$ and $c = 1000$ were calculated. $\delta_e - \delta_a$ values at these extreme values of c were then used as lower and upper limits for the extrapolated shifts.

One parameter that is unobtainable and needed in the fast-exchange region is the IIE. In principle, this value can be obtained in the slow-exchange region and then extrapolated to higher temperatures. However, this can only be done if the axial and equatorial C—H resonances are sharper than the chemical shift difference between the CH_2 and CHD proton peaks in slow-exchange. At low temperatures, the axial and equatorial C—H peaks have a linewidth of approximately 15 Hz, probably due to nuclear dipole–dipole broadening. Because the linewidth of the axial and equatorial C—H peaks is larger than the IIE, it is difficult to measure the IIE for CHT-7-*d* in the slow-exchange region. The smallest known value (for sp^3-hybridized carbon atoms) for such an IIE is -15 ppb for methane,[39] and the largest is -22 ppb for the CH_2 at C5 in 2,2-dimethyl-5-*d*-1,3-dithiane.[28] The two-bond IIE in CHT-7-*d* could not be measured experimentally, and we use a shift, Δ_{int}, of -18 ppb as a reasonable estimate of the intrinsic isotope effect in CHT-7-*d*.[15,16,28] It is worth noting that the value of Δ_{int} is small and not substantially temperature dependent.[39] Errors in Δ_{int} were assumed to be ± 4 ppb.

The following analysis is based on the assumption that only CHT is present in solution. Previous studies indicate that anywhere from 0.002%[3] to 0.1%[2] NCD may be present at room temperature; but a recent report suggests that as much as 2% NCD may be present at room temperature.[4] This corresponds to 0.4% NCD at -60 °C. The relative amount of NCD in solution should decrease with decreasing temperature, and should not affect the measured chemical shifts of CHT. Thus the presence of 0.4% NCD or less in the NMR tube should yield accurate values of K_{eq}.

Equilibrium constants in $CBrF_3$ and $CClF_2H$ resulting from substitution of the extrapolated $\delta_e - \delta_a$ substituted into Eqn. (9), together with the measured $\Delta\delta$ values, are shown in Table 2. Fast-exchange data in both solvents yield $\Delta G°$ values similar to those obtained in the slow-exchange region by direct integration in $CBrF_3$ (see Table 1). Reliable thermodynamic parameters in the fast-exchange region were obtained from Eqn. (9) using $\delta_e - \delta_a$ values extrapolated from NMR spectra taken in the slow-exchange in $CBrF_3$ and $CClF_2H$. As a result, the high-temperature equilibrium constants in this investigation differ from those reported by Jensen and Smith.[12] Figure 6 shows a plot of $\Delta G°$ versus temperature (in $CBrF_3$) obtained in the present study and data reported by Jensen and Smith.[12] There is good agreement between $\Delta G°$ values obtained in $CClF_2H$ and those in $CBrF_3$ in the fast-exchange region (Table 2). Significantly, Fig. 6 shows a small $\Delta S°$ for measurements obtained in the present study, and a larger $\Delta S°$ obtained by Jensen and Smith.[12] The magnitude of $\Delta S°$ is important because, in Jensen and Smith's study,[12] it predicts that the deuterium conformational preference changes from equatorial to axial above 191 K. In the present study, fast-exchange equilibrium constants were calculated using extrapolated chemical shift differences, accounting for temperature dependence in the axial-H equatorial-H chemical shift difference. Combining and fitting the slow- and fast-exchange free-energies yields $\Delta H°$ and $\Delta S°$ in $CBrF_3$ of 55 ± 8 cal mol^{-1} and 0.03 ± 0.05 cal mol^{-1} K^{-1} respectively. $\Delta G°$ values obtained in the fast-exchange region are similar to those measured by integration at lower temperatures, and imply that $\Delta G°$ is only weakly

Table 3. Calculated geometric parameters for the boat form of CHT at various levels of theory

Level of theory	Distance (Å)			Lowest two vibrational frequencies (cm^{-1})[a]
	C1—C6	C7—H_{ax}	C7—H_{eq}	
RHF/3-21G	2.458	1.086	1.081	211, 291
RHF/6-31G*	2.480	1.088	1.083	186, 287
RHF/6-311G*	2.480	1.088	1.083	185, 286
MP2/6-31G*	2.390	1.099	1.093	236, 276

[a] The RHF frequencies are scaled by 0.90; the MP2 frequencies are scaled by 0.95.[40]

Table 4. Calculated scaled stretching frequencies for the axial and equatorial C—D bonds in CHT-7-*d*

	RHF/3-21G[a]	RHF/6-31G*[a]	MP2/6-31G*[a]	Experimental[11]
Axial C—D (cm^{-1})	2115 (2351)	2111 (2346)	2133 (2270)	2125
Equatorial C—D (cm^{-1})	2158 (2398)	2157 (2397)	2187 (2327)	2183
$\Delta\nu$ (cm^{-1})	43 (48)	46 (51)	54 (57)	58

[a] Values given in parentheses are unscaled vibrational frequencies.

temperature dependent. These results disagree with those of Jensen and Smith[12] and show that $\Delta S°$ for an isotopically perturbed equilibrium should be very close to zero for a system such as this.[28,29]

Ab initio calculations

To obtain an independent measure of the isotope effect in CHT-7-*d*, *ab initio* calculations were carried out. At all levels of theory considered, *ab initio* calculations showed the C_s boat conformation to be an energy minimum on the potential energy surface with only real (not imaginary) vibrational frequencies. The C_{2v} planar-ring form was calculated to be a transition state for ring inversion (one imaginary frequency). The lowest calculated vibrational frequencies (C_s form) are listed in Table 3; the calculated stretching vibrational frequencies can be found in Table 4. Overall, the difference in axial and equatorial C—D stretching frequencies is approximately 50 cm^{-1}, which corresponds to a $\Delta H°_{str}$ value of approximately 25 cal mol^{-1}. The experimentally determined $\Delta H°$ is 55 cal mol^{-1}, leaving 30 cal mol^{-1} for bending contributions to the overall $\Delta H°$. These calculated (scaled) stretching frequency differences reproduce the experimentally observed values to within 7%.[11] Owing to neglect of electron configuration interaction and vibrational anharmonicity, vibrational frequencies calculated at the RHF level are systematically higher than the observed experimental vibrational frequencies.[4,35,40]

Table 5 summarizes the thermodynamic parameters calculated at the RHF/3-21G, RHF/6-31G* and MP2/6-

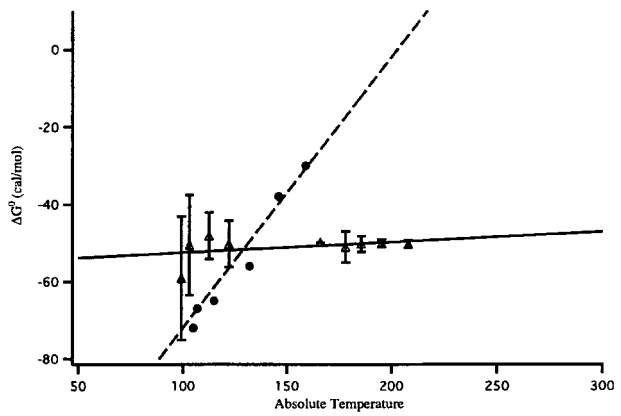

Figure 6. A comparison of thermodynamic data obtained in different solvents: plot of least-squares fit of $\Delta G°$ versus absolute temperature for CHT-7-*d* in $CBrF_3$ (solid line), $\Delta G°$ versus absolute temperature, in kelvin, for CHT-7-*d* with integration data from $CBrF_3$ and Jensen and Smith's data (broken line).[12] Fitting the linear free-energy relation yields $\Delta H° = 55 \pm 8$ cal mol^{-1} and $\Delta S° = 0.03 \pm 0.05$ cal mol^{-1} K^{-1} for $CBrF_3$. Plotted for comparison are Jensen and Smith's data,[12] reported as $\Delta H° = 142 \pm 30$ cal/mol^{-1} and $\Delta S° = 0.7$ cal mol^{-1} K^{-1}

Table 5. Summary of *ab initio* calculations of isotope effects in CHT-7-*d* (see Fig. 2)

Level of theory	Temperature (K)	$\Delta H°$ (cal mol^{-1})	$\Delta S°$ (cal mol^{-1} k^{-1})
RHF/3-21G	77	+ 38	−0.026
	200	+ 42	+0.015
	298.15	+ 44	+0.021
RHF/6-31G*	77	+ 49	−0.020
	200	+ 55	+0.024
	298.15	+ 57	+0.029
MP2/6-31G*	77	+ 29	−0.027
	200	+ 35	+0.015
	298.15	+ 34	+0.014

Table 6. Comparison of calculated and experimental moments of inertia in CHT

	(amu Å^2)			
Moments of inertia	RHF/6-31G* geometry	Average of MP2 and RHF geometry	MP2/6-31G* geometry	Experimental[9]
I_a	136.2212	136.2072	136.1932	136.7736
I_b	137.6722	137.0182	136.3641	137.6683
I_c	251.2073	248.3037	245.400	248.748

31G* levels. $\Delta H°$ at the RHF levels is fairly consistent, yielding values between 38 and 57 cal mol^{-1}, depending on temperature. The MP2/6-31G* calculations yield systematically lower values of $\Delta H°$ than the RHF levels, but this may be accidental. Importantly, the overall $\Delta S°$ is nearly zero at the RHF and MP2 levels. To calculate the overall $\Delta S°$, only the rotational and vibrational entropy contributions are needed. Differences in the rotational entropy in CHT-7-*d* are entirely due to differences in the moments of inertia in the two conformers. Interestingly, the calculated overall value of $\Delta S°$ shows a distinct temperature dependence: the rotational entropy $\Delta S°_{rot}$and the vibrational entropy $\Delta S°_{vib}$,are opposite in sign (supplementary table S2). At low temperatures, only the lowest vibrational level is populated, yielding a very small value for the vibrational entropy; the rotational entropy, however, remains constant even over a temperature range of 200 °C. An increase in temperature increases the number of populated vibrational levels, thus increasing the vibrational entropy, and offsetting the rotational entropy. Nevertheless, the total calculated $\Delta S°$ is very close to zero, and has only a slight temperature dependence.

It is possible that the anharmonicity of the potential energy surface (PES) in CHT may affect calculation of $\Delta H°$ and $\Delta S°$,[41] but these calculations are computationally expensive and may be the subject of a separate study. However, an important conclusion of Kopelevich's work is that $\Delta H°$ and $\Delta S°$ could be accurately calculated even at low levels of theory, assuming a harmonic PES when differences or differences of differences are taken.[29] Additionally, the main contribution to the isotope effect arises due to the difference in the high-frequency modes, and anharmonicity is expected to have a small effect on this difference.

Calculated moments of inertia in the present study agree closely with experimentally determined values[9] (Table 6). The calculated values for I_a and I_b at the RHF/6-31G* level of theory more closely match the experimental than the I_a and I_b calculated at the MP2/6-31G* level of theory. However, the experimental value for I_c, which is extremely sensitive to the degree of ring nonplanarity in CHT, falls between the MP2/6-31G* value and the RHF/6-31G* value. It appears that I_c is overestimated at the MP2/6-31G* level of theory and somewhat underestimated at the RHF/6-31G* level of theory. Structures of CHT inferred from electron diffraction[8] and those inferred from microwave data[9] are distinguishable based on their significantly different moments of inertia. The data obtained for this investigation[28] are in agreement with the CHT structure inferred from microwave data. Notably, results obtained from calculations by Gajewski and co-workers[4] and Radom and co-workers[42] are consistent with experimental data inferred from microwave spectra.[9] Together with our data,[28] these two separate reports[4,42] of the calculated moments of inertia provide independent support for a C1—C6 distance that is somewhat shorter than the one calculated at the RHF level.

Table 7 shows the calculated potential energy barrier for ring inversion in CHT. These data indicate that at the RHF level, the calculated ring-inversion barrier for CHT (4 kcal mol^{-1}) reproduces the experimental barrier of approximately 6 kcal mol^{-1} with only fair accuracy. When second-order perturbation theory is used to calculate the ring-inversion barrier, it suddenly jumps to 10 kcal mol^{-1}. This large change in barrier height is likely due to stabilization from orbital overlap between C1 and C6, which is overestimated at the MP2/6-31G* level of theory. However, this increased stabilization in the boat form of CHT alone cannot explain why the potential energy barrier suddenly became 10 kcal mol^{-1}. In order to understand this effect better, a series of single-point calculations at the MP4/6-31G* level of theory was carried out. The single-point energies of the C_{2v} form, and the boat C_s form at MP4/6-31G* were calculated using coordinates optimized at RHF/6-31G* and MP2/6-

Table 7. Ring-inversion barrier for CHT calculated at various levels of theory

Level of theory	Calculated potential energy barrier (kcal mol^{-1})
RHF/6-31G*	4.26
MP2/6-31G*	9.76
MP4/6-31G*[a]	7.10
MP4/6-31G*[b]	7.34
MP4/6-31G*[c]	7.17

[a] Potential energy barrier calculated using geometry optimized at RHF/6-31G*.
[b] Potential energy barrier calculated using average geometry from RHF/6-31G* and MP2/6-31G*.
[c] Potential energy barrier calculated using geometry optimized at MP2/6-31G.

31G*. Optimized RHF/6-31G* and MP2/6-31G* coordinates for the C_s form of CHT were averaged to generate an additional geometry used in the MP4/6-31G* single-point calculation. Single point MP4/6-31G* calculations on the planar C_{2v} (transition-state) geometry of CHT used the same coordinates that were obtained in the MP2/6-31G* calculations. The coordinates for planar CHT calculated at the RHF/6-31G* level were nearly identical to those obtained at the MP2/6-31G* level. Table 7 shows results from the MP4/6-31G* single-point calculations. At MP4/6-31G* the calculated potential energy barrier using optimized RHF/6-31G* and MP2/6-31G* structures is 7.3 kcal mol^{-1}, in good agreement with the experimental barrier. The larger calculated barrier height at the MP2/6-31G* level may be due to an overestimation of the energy of the planar-ring form of CHT together with an underestimation of the boat form of CHT. The results obtained for this investigation[28] are in agreement with recent reports, which find that the barrier to ring-inversion in CHT is between 4.3 and 9.8 kcal mol^{-1} from *ab initio* calculations,[42] and 5.2 kcal mol^{-1} from density functional theory calculations.[4] These reports did not investigate the variation in ring-inversion barrier, with respect to level of theory. We therefore explore this effect below.

Table 3 shows some important features of calculated bond distances and interatomic distances. The equatorial C—H bond for the methylene group in CHT is calculated to be shorter than the axial bond by approximately 0.005 Å, regardless of the choice of basis set. This observation is consistent with the experimental observation that the equatorial bond has a larger force constant than the axial bond. Table 3 also shows an interesting trend in the interatomic C1—C6 distance on going from the RHF to the MP2 level of theory. Smaller basis sets without perturbation yield a fairly constant C1—C6 distance of approximately 2.48 Å. Introduction of second-order Møller–Plesset perturbation theory yields a C1—C6 distance of 2.39 Å, a decrease of 4%. Although some variation in bond length is expected from calculations at different levels of theory, the change in the C1—C6 distance is substantial and is understandable in terms of homoconjugation.[6] Homoconjugation makes CHT homoaromatic, which biases the structure of CHT toward NCD, depending on the degree of orbital overlap between C1 and C6. The degree of orbital overlap depends on the balance between an increase in strain energy of the newly formed ring and the decrease in its electronic energy. With MP2, electron excitation to virtual molecular orbitals is computed. The low-lying unoccupied (virtual) molecular orbital in CHT has bonding character between C1 and C6. When electron density in this molecular orbital is allowed to mix with electron density in the highest occupied molecular orbitals, the result is a CHT structure with some NCD character.[43] Hence, if homoconjugation is an important feature in CHT, a decrease in the interatomic C1—C6 distance is expected, and this effect is observed at MP2/6-31G*. Together with the change in barrier to ring inversion upon using MP2, a shorter C1—C6 distance and smaller C1—C7—C6 bond angle of approximately 105°[4] can be explained in terms of neutral homoconjugation, even though the effects of homoaromaticity in electronically neutral molecules are thought to be weak.[44] Our results show that homoaromaticity in CHT may be detectable, and have implications for the CHT–NCD equilibrium and the ring-inversion equilibrium of CHT. The ground state of CHT is stabilized by the p orbital overlap of C1 and C6, and the barrier to ring inversion is increased as a result. At the same time, the overlap distorts CHT so that the six-membered ring is somewhat flattened, and has some geometrical characteristics of NCD.

The *ab initio* results from various levels of theory provide similar structures for CHT, indicating that the calculated structure of CHT is reproducible. Although *ab initio* calculations provide a geometry for CHT, there is no low-temperature X-ray crystal structure of CHT that can be used to compare with the calculated molecular geometry of CHT. There is, however, an X-ray crystal structure of thujic acid, which shows a C1—C6 distance of 2.41 Å,[10] in line with the C1—C6 determined in our *ab initio* studies. It would also be desirable to use *ab initio* calculations to fit the entire vibrational spectrum of CHT, as has been done for cyclopentene.[45]

CONCLUSIONS

We have measured the conformational preference for the deuterium in CHT-7-*d* over a wide temperature range using three independent methods: Saunders' isotopic perturbation method[17–20,46–50] in conjunction with integration in the slow-exchange region and lineshape analysis in the intermediate-exchange region. The CHT equilibrium is skewed, with a conformational preference for deuterium in the equatorial position by 52 ± 8 cal mol^{-1} at -173 °C, with $\Delta H° = 55 \pm 8$ cal mol^{-1} and $\Delta S° = 0.03 \pm 0.05$ cal mol^{-1} K^{-1} in $CBrF_3$. Although the $\Delta G°$ values reported by Jensen and Smith[12] in 1964 are essentially correct, the present results clearly establish that the thermodynamic data, which provided $\Delta H° = 142 \pm 30$ cal mol^{-1} and $\Delta S° = 0.7 \pm 0.3$ cal mol^{-1} K^{-1}, for CHT-7-*d* are in error. The difficulty of obtaining reliable values for $\Delta H°$ and $\Delta S°$ arises because these parameters were calculated from the temperature dependence of $\Delta G°$ over a limited temperature range (54° in Jensen and Smith's case). The NMR work described in this paper has been done over a wider temperature range (110 °C) using more modern instruments and methodologies, which avoid the introduction of systematic errors in obtaining equilibrium constants and free energy differences. The results obtained from the NMR measurements also agree with those from *ab initio* quantum mechanical calculations, which show $\Delta H° = 55$

cal mol^{-1} (RHF/6-31G*) and $\Delta S° = 0.02$ cal mol^{-1} K^{-1} at room temperature. The experimental values for $\Delta S°$ are very accurate, extremely small, and the calculated values show a distinct temperature dependence. The $\Delta H°$ of approximately 34 cal mol^{-1} calculated at the MP2 level does not agree with our experimental results; however, the theoretical and experimental values may be in closer agreement at higher levels of theory. Our experimental findings are further confirmed by quantum mechanical *ab initio* calculations, which show that the major contribution to the overall $\Delta S°$ originates from the zero-point vibrational energy level difference between the conformers having an axial and an equatorial deuterium. Our calculations also agree with the IR data measured by la Lau and de Ruyter[11] that predict a 25 cal mol^{-1} difference in the stretching contribution to $\Delta H°$. This report shows that a combination of low-temperature integration and measurements of high-temperature equilibrium isotope effects on the chemical shift provide a general framework for accurate measurements of isotope effects.

Acknowledgements

We wish to thank Dan O'Leary for helpful discussions and for making available thermodynamic results of RHF/3-21G calculations for CHT, Peggy Thompson and Richard Pastor for a thorough reading of the manuscript, and Jane Strouse for assistance with NMR spectrometers.

REFERENCES

1. Ladenburg A. *Liebigs Ann. Chem.* 1883; **217**: 74.
2. Rubin M. *J. Am. Chem. Soc.* 1981; **103**: 7791.
3. Miura S. *Ph.D. Dissertation*, University of California, Los Angeles, 1984.
4. Jarzecki AA, Gajewski J, Davidson ER. *J. Am. Chem. Soc.* 1999; **121**: 6928.
5. Alder K, Jacobs G. *Chem. Ber.* 1953; **86**: 1528.
6. Winstein S. *J. Am. Chem. Soc.* 1959; **81**: 6524.
7. Corey EJ, Burke HJ, Remers WA. *J. Am. Chem. Soc.* 1955; **77**: 4941.
8. Traetteberg M. *J. Am. Chem. Soc.* 1964; **86**: 4265.
9. Butcher SS. *J. Chem. Phys.* 1965; **42**: 1833.
10. Davis RE, Tulinsky A. *Tetrahedron Lett.* 1962; **19**: 839.
11. la Lau C, de Ruyter H. *Spectrochim. Acta* 1963; **19**: 1559.
12. Jensen FR, Smith LA. *J. Am. Chem. Soc.* 1964; **86**: 956.
13. Anet FAL. *J. Am. Chem. Soc.* 1964; **86**: 458.
14. Siehl H-U. In *Isotope Effects on the NMR Spectra of Equilibrating Systems,* Webb, G (ed.). Academic Press: London, 1987; 63–163.
15. Hansen PE. In *Isotope Effects on Nuclear Shielding*, Emsley, JW, Feeney, J, and Suttcliffe, LH (eds). Academic Press: London, 1983; 106–234.
16. Hansen PE. *Prog. NMR Spec.* 1988; **20**: 207.
17. Saunders M, Vogel P. *J. Am. Chem. Soc.* 1971; **93**: 2561.
18. Saunders M, Jaffe MH, Vogel P. *J. Am. Chem. Soc.* 1971; **93**: 2558.
19. Saunders M, Vogel P. *J. Am. Chem. Soc.* 1971; **93**: 2561.
20. Saunders M, Kates MR. *J. Am. Chem. Soc.* 1980; **102**: 3571.
21. Anet FAL, Kopelevich M. *J. Am. Chem. Soc.* 1986; **108**: 2109.
22. Anet FAL, Kopelevich M. *J. Am. Chem. Soc.* 1986; **108**: 1355.
23. Anet FAL, Kopelevich M. *J. Chem. Soc. Chem. Commun.* 1987; 595.
24. Forsyth DA, Hanley JA. *J. Am. Chem. Soc.* 1987; **109**: 7930.
25. Anet FAL, O'Leary DJ. *J. Am. Chem. Soc.* 1989; **111**: 8935.
26. Forsyth DA, Prapansiri V. *J. Am. Chem. Soc.* 1989; **111**: 4548.
27. Anet FAL, O'Leary DJ, Williams PG. *J. Chem. Soc. Chem. Commun.* 1990; **20**: 1427.
28. Freedberg DI. *Ph.D. Dissertation*, UCLA, 1994.
29. Kopelevich M. *Ph.D. Dissertation*, UCLA, 1987.
30. Conrow K. *J. Am. Chem. Soc.* 1961; **83**: 2349.
31. Van Geet AL. *Anal. Chem.* 1970; **42**: 679.
32. Marion D, Bax A. *J. Magn. Reson.* 1988; **79**: 352.
33. Neuhaus D, Williamson M. *The Nuclear Overhauser Effect in Structural and Conformational Analysis*. VCH: New York, 1989.
34. Sandström J. *Dynamic NMR Spectroscopy*. Academic Press: London, 1982.
35. Frisch MJ, Trucks GW, Head-Gordon M, Gill PMW, Wong MW, Forseman JB, Johnson BG, Schlegel HB, Robb MA, Replogle ES, Gomperts R, Andres JL, Ragavachari K, Binkley JS, Gonzalez RL, Martin RL, Fox DJ, Defrees DJ. Gaussian, Pittsburgh, 1992.
36. Bigeleisen J, Mayer MG. *J. Chem. Phys.* 1947; **15**: 261.
37. Bevington PR. *Data Reduction and Analysis for the Physical Sciences*. McGraw-Hill: New York, 1969.
38. Wavemetrics. Igor Pro, Lake Oswego, 1994.
39. Anet FAL, O'Leary DJ. *Tetrahedron Lett.* 1989; **30**: 2755.
40. Pople JA, Scott AP, Wong MW, Radom L. *Isr. J. Chem.* 1993; **33**: 345.
41. Carcabel P, Brenner V, Halberstadt N, Millie P. *Chem. Phys. Lett.* 2001; **336**: 335.
42. Scott AP, Agranat I, Biedermann PU, Riggs NV, Radom L. *J. Org. Chem.* 1997; **62**: 2026.
43. Hoffman R. *Tetrahedron Lett.* 1970; **33**: 2907.
44. Williams RV, Kurtz HA. *Adv. Phys. Org. Chem.* 1994; **29**: 273.
45. Allen WD, Császár AG, Horner DA. *J. Am. Chem. Soc.* 1992; **114**: 6834.
46. Saunders M, Kates M, Telkowski L. *J. Am. Chem. Soc.* 1977; **99**: 8070.
47. Saunders M, Kates M, Wiberg K, Pratt W. *J. Am. Chem. Soc.* 1977; **99**: 8072.
48. Saunders M, Telkowski L, Kates M. *J. Am. Chem. Soc.* 1977; **99**: 8071.
49. Saunders M, Siehl H-U. *J. Am. Chem. Soc.* 1980; **102**: 6868.
50. Saunders M, Kates MR. *J. Am. Chem. Soc.* 1980; **102**: 6867.